Monotonic and cyclic pull-pull tests on dowel-nut connector in laminated veneer lumber made of European beech wood

Andrea FABBRI, Fabio MINGHINI[a], Nerio TULLINI

Department of Engineering, University of Ferrara, Italy.

[a]corresponding author; e-mail: fabio.minghini@unife.it

GRAPHICAL ABSTRACT

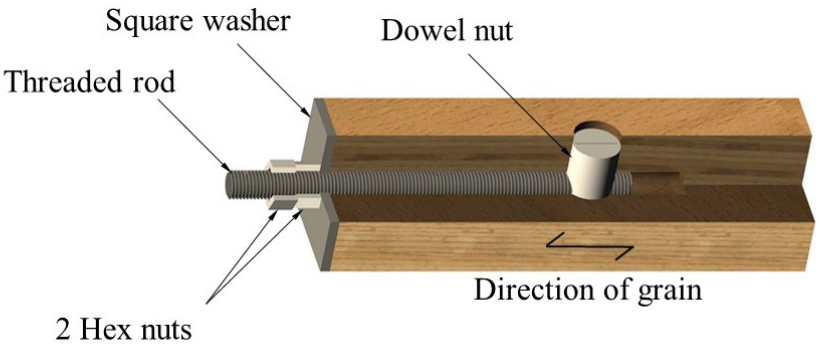

ABSTRACT

The findings from tests on steel dowel-nut connector in Laminated Veneer Lumber (LVL) bar are reported. Test specimens were prepared using LVL members made of European beech wood (*Fagus sylvatica L.*), showing a square cross-section of side length 50 mm and veneers arrangement comprised of 18 layers with the grain oriented in the bar longitudinal direction. The tested connection consisted in a 12 mm-diameter longitudinal threaded rod of class 12.9 steel (nominal yield strength f_{yb} = 1080 MPa) screwed into a transverse 20 mm-diameter (= d), 50 mm-long dowel-nut. Three monotonic compression tests and 42 pull-pull tests were carried out. Among these latter, 22 were monotonic and the remaining 20 were cyclic. The dowel-nuts were also made of class 12.9 steel, with the exception of those used in ten cyclic tests, which were of grade S355 steel (f_{yk} = 355 MPa).

Preloading the connection with a controlled tightening increased both tension and compression stiffness. Greater tensile strength and smaller results scatter were found for dowel-nut axis orthogonal to the veneers. Load-carrying capacities obtained for dowel-nut end distances of 2.5*d* and 5*d* were 33% and 100%, respectively, those obtained for 7.5*d*. In cyclic tests, no significant increase in the strength degradation was observed due to cyclic loading. In the case of grade S355 dowel-nut, evident plastic deformations were achieved in the connector for end distances 5*d* and 7.5*d*. However, this did not influence neither strength nor corresponding displacement.

Keywords: Dowel-nut; Bed-bolt nut; Barrel bolt; Larsen bolt; Beech; LVL; Monotonic test; Cyclic test; Pull-pull test; Preload; Tightening.

1. INTRODUCTION

In structural applications, timber offers the opportunity to pursue sustainable solutions with low environmental and economic impact. For this reason, the use of timber is increasingly explored even for the restoration of earthquake damaged buildings. For example, in unreinforced masonry buildings, strengthening existing timber floors and their connections to the walls allows reducing, at relatively low costs, the risk of out-of-plane collapses [1]. Timber can also be used for the reconstruction or retrofitting of industrial buildings in seismic areas. In this context, after the 2012 Emilia (Italy) earthquakes, in addition to the use of traditional technologies based on precast reinforced concrete [2] or steel [3], low impact lightweight solutions based on wood products were frequently adopted for long span roofs and cladding [4]. With regard to timber truss structures, the connections are often governing the entire structural design and represent both technical and economic limits for conventional construction [5]. Some prototype of innovative timber [6] or timber and steel hybrid spatial truss structure [7] was recently proposed and tested, but opportunities still remain for the development of efficient joint solutions.

Through-bolt with steel dowel-nut connectors are commonly used in furniture [8−10], particularly in the connection of the side rail to the back post of a chair, the attachment of the wooden table leg to table top, and the connection of bed rails to bed posts, where terms barrel nut or bed-bolt nut connectors are usually used. This type of joint is characterized by high strength and low visual impact; thus, several researches proposed through-bolt with dowel-nut connectors as end connections for round wood frame construction [5, 6, 11−13]. A withdrawal capacity greater than 89 kN was obtained in [11] for 38.1 mm-diameter dowel-nuts in 150 to 175 mm-diameter yellow poplar peeler cores. In [12], a 44.5 mm-diameter dowel-nut connector appears to be economically feasible at a design capacity of 44.5 kN for a 127 mm-diameter Douglas-fir peeler core (mean density 400 kg/m^3). In [13], the failure of a 30-mm diameter dowel-nut in 91 to 140 mm-diameter Portuguese forest maritime pine poles (mean density 558 kg/m^3) was caused by splitting of the

wood at a mean load of 95 kN. For those dowel-nut connections, the European Yield Model formulation provided good estimates of the load-carrying capacity.

Despite these preliminary results, through-bolt with dowel-nut connectors have had only limited use in conventional timber frame construction. This may probably be due to the high-precision manufacturing process required to ensure the correct mutual position of longitudinal and transversal holes. Another reason could be related with costs of dowel-nuts, for which galvanized or stainless steels are required to avoid corrosion.

Also little frequent appears the constructional use of Laminated Veneer Lumber (LVL), particularly if made of beech wood, despite the interesting potentialities showed by this material. European beech (*Fagus sylvatica L.*) is the main hardwood species, in terms of the volume of young stems, present in Central European forests [14]. Industrialized production of beech LVL yields reliable high strength and stiffness properties as well as improved dimensional and form stability. Several studies [15−19] have demonstrated the potential of beech LVL for structural applications, highlighting its favorable mechanical properties. In particular, dowel-type connections with beech LVL enable high load-bearing capacities and ductile slip [17−19]. However, the use of beech LVL remains quite sporadic just because of its high strength, which cannot always be completely exploited due to the limiting resistance of the joints.

Aiming at exploring the feasibility of a double layer grid structure comprised of beech LVL bars and pin-joint connections in steel ball nodes having an adequate number of threaded holes, this paper reports findings from monotonic and cyclic pull-pull tests on threaded rod with dowel-nut connector in beech LVL square section bars. In all experimental tests, the applied axial force was parallel to grain of the beech LVL bar. Test specimens were prepared using LVL members made of European beech wood (*Fagus sylvatica L.*), showing a square cross-section of side length 50 mm and veneers arrangement comprised of 18 layers. The tested connection consisted in a 12 mm-diameter longitudinal threaded rod of class 12.9 steel (nominal yield strength f_{yb} = 1080 MPa)

screwed into a transverse 20 mm-diameter (= d), 50 mm-long dowel-nut. Three monotonic compression tests and 42 pull-pull tests were carried out. Among these latter, 22 were monotonic and the remaining 20 were cyclic. The dowel-nuts were also made of class 12.9 steel, with the exception of those used in ten cyclic tests, which were of grade S355 steel (f_{yk} = 355 MPa).

During the lifetime of a double layer grid structure, a generic bar may be subjected to both tensile and compressive axial loads having almost the same intensity, mainly due to wind or vertical earthquake actions. Thus, the joint has to be able to sustain an axial force in both tension and compression. To this end, an adequate square washer was placed at the wood element end, and a preloading in the form of a controlled tightening torque was assigned to the threaded rod with dowel-nut connector. It is worth remember that buckling failure regulates the design of slender compressed bar; thus, no joint failure due to compressive force deserves to be analyzed. Nonetheless, a couple of monotonic tests with compressive load were performed to show the importance of preloading the dowel-nut connection.

Monotonic tests were performed with the axis of the dowel-nut either parallel or orthogonal to the veneer layers. For cyclic tests, only the latter configuration was adopted, as in monotonic tests it yielded the smaller Coefficient of Variation (CoV) of the load-carrying capacity. During the tests the load-displacement curve of the dowel-nut connection relatively to the LVL bar was measured.

Finally, the application to this connection of design equations based on the European Yield Model (see [20]) is discussed.

The whole experimental results are provided in specific data sheets as supplementary material, to which the interested reader is referred to.

2. MATERIALS, SPECIMENS AND METHODS ADOPTED IN THE EXPERIMENTAL TESTS

The materials involved in this research are presented herein, followed by a description of test specimens and methods adopted for the characterization of stiffness, failure modes, displacement and load-carrying capacities of the connector.

2.1. LVL made of European beech

The LVL material used in the present research was produced by company Pollmeier GmbH & Co. KG in Creuzburg, Germany. It was manufactured from 3.0 mm thick rotary-peeled beech veneers. In the manufacturing process the veneers were compressed to a thickness of about 2.8 mm. The mean mass density (see Table 1) obtained from measurements on 8 specimens resulted to be of 843 kg/m^3 (CoV = 2.5%). The cross-sectional layout consisted in veneers oriented with the grain parallel to the longitudinal direction of the LVL member. No cross-layer was present.

In the experiments, LVL bars having square cross-section with side length of 50 mm and comprised of 18 veneers were considered. Table 1 reports material and mechanical properties of beech LVL based on manufacturer's data and experimental tests. Moisture content was 8 ± 2%, which represents the climatic conditions of the indoor use of beech LVL.

2.2. Threaded rod with steel dowel-nut connector

The connection considered in the experimental tests (Fig. 1) consisted in a threaded rod and a smooth dowel-nut inserted into a longitudinal and a transverse hole, respectively (Fig. 2a). The longitudinal hole was centered along the wood element axis, whereas the transverse one was placed at end distance a_1 and lateral edge distance a_2. The dowel-nut presented a transverse threaded hole at midpoint, needed for screwing the threaded rod. Both rod- and nut-hole clearance was of 1 mm. Then, the connection assembly (Fig. 2b) required a high-level precision for the correct positioning of the connector. A square washer, with side length and thickness of 50 and 4 mm, respectively, was placed at the LVL bar end section, whereas two hexagonal nuts, in contact with each other (Fig.

2c), allowed screwing the threaded rod into the dowel-nut. Once the connection was assembled (Fig. 2d), a preload in the form of a controlled tightening torque was assigned to the threaded rod with dowel-nut connector acting on the hexagonal nut in contact with the square washer. Finally, the outer hexagonal nut was screwed up to reobtain contact with the other nut and secure the connection.

2.3. Characteristics and designation of test specimens

In all of the tests, a metric 12 mm-diameter, class 12.9 threaded rod (nominal yield and ultimate tensile strengths f_{yb} = 1080 MPa and f_{tb} = 1200 MPa, respectively) was used. This avoided yielding of the threaded rod. Moreover, smooth dowel-nuts with diameter d = 20 mm and length l = 50 mm were adopted. To evaluate the influence of connector yield strength, the dowel-nuts used for cyclic load tests were obtained from either grade S355 bars (f_{yk} = 355 MPa, f_{tk} = 510 MPa) or class 12.9 threaded rods with nominal diameter of 24 mm, which were subjected to cutting and turning lathe machining operations.

Edge distance a_2 perpendicular to the wood element axis was equal to 25 mm (= 1.25d), smaller than the minimum non-loaded edge distance of 3d prescribed in [20]. Moreover, three values of end distance a_1 parallel to the wood element axis, equal to 50 mm (= 2.5d), 100 mm (= 5d) and 150 mm (= 7.5d), were tested. It is worth noting that only this latter complies with the minimum loaded end distance of 7d prescribed in [20].

Various preloading forces were also compared in monotonic tests. They were applied to the threaded rod with steel dowel-nut connector by means of a controlled tightening torque M_t of 0, 20, 40 and 80 Nm. The reader is referred to Table 2 for the value of M_t applied to each of the tested specimens. In cyclic tests, a tightening torque of 40 Nm was adopted, corresponding to approximately 1/3 and 1/6 of the torques producing failure of the connection for an end distance of a_1 = 50 and 100 mm, respectively.

A symmetric test layout with two equal end connections was adopted for each specimen. In this configuration, the distance of the dowel-nuts from one another always was greater than 500 mm (i.e., 10 times the side length of the LVL member cross-section). Therefore, it can reasonably be assumed that a uniform stress distribution took place in the intermediate part of each specimen, with no influence of the end connections on one another. The results presented in the following refer, for each specimen, to the connection which reached failure.

Monotonic pull-pull tests were performed with the axis of the dowel-nut either parallel or orthogonal to the veneer layers. Due to the larger mean values and smaller CoVs of load-carrying (peak) capacity F_{peak} obtained from monotonic tests on specimens with dowel-nut axis orthogonal to the veneers (see Sect. 4), in cyclic pull-pull tests such dowel-nut orientation was investigated only. To identify each test, the following label is used:

Wood species - LVL side length - Dowel-nut grade - Test type - a_1 - Test number,

where:

- Wood species = B (indicating Beech);
- LVL side length = 50 mm (note that species and LVL side length are invariant in this research; nonetheless, they are reported in the label in view of subsequent researches on other species and different cross-section dimensions);
- Dowel-nut grade = 12.9 or S355;
- Test type is identified by means of an acronym related with loading protocol (i.e., monotonic, "M", or cyclic, "C"), load direction (i.e., tension, "T", or compression, "C") and dowel-nut axis orientation with respect to the veneer layers (i.e., parallel, "P", or orthogonal, "O"). For tension-compression cyclic tests, the acronym part related with the load direction is dropped for simplicity of notation. The following alternatives were then considered: MCO (monotonic compression test with dowel-nut axis orthogonal to the veneer layers), MTP (monotonic pull-pull test with dowel-nut axis parallel to the veneer layers), MTO (monotonic pull-pull test with

dowel-nut axis orthogonal to the veneer layers), CTO (cyclic pull-pull test with dowel-nut axis orthogonal to the veneer layers, where only tensile load was applied), and CO (cyclic test with dowel-nut axis orthogonal to the veneer layers, where both compressive and tensile loads were applied, but failure occurred in tension);

- a_1 = 50, 100 or 150 mm (see Fig. 1);
- Test number = 1, ..., 4.

2.4. Loading protocols and measuring system

The principal purpose of this research was to characterize the connector behaviour in tension. Consequently, the monotonic pull-pull tests, i.e., MTP and MTO, were carried out in accordance with the loading protocol reported in [23]. Nonetheless, cyclic tests were useful to assess the influence of alternate loads on tension damage of the connector. Thus, for CO cyclic tests the loading protocol was defined to always obtain failure in tension and to achieve a maximum compressive load less than or equal to the expected failure load in tension. In tests with a_1 = 50, 100 and 150 mm the compressive load was limited to about 20, 40 and 45 kN, respectively, decided on the basis of the minimum tensile strengths obtained from MTO tests. To explore the effects due to higher compressive stresses, maximum target compressive loads of 50 and 60 kN were adopted for specimens B-50-S355-CO-100-2 (a_1 = 100 mm) and B-50-S355-CO-150-3 (a_1 = 150 mm), respectively. Future experimental tests will be focused on the compression failure of LVL struts and possible interaction between strut buckling and joint collapse.

The cyclic loading protocol reported in [24], based on displacement control with target displacements which are submultiples and multiples of the joint yield displacement, was considered impractical for two reasons. First, according to the procedure outlined in [24], the so-called yield displacement depends on the slope gradient of the monotonic force-displacement behaviour, and for the specimens tested in this research would lead to some inconsistencies from case to case. Second, a displacement control with equal target displacements in tension and compression would make no

sense due to significant differences in tension and compression stiffnesses of the connection. Therefore, the adopted procedure was based on displacement control in tension and load control in compression. In particular, in tension, target displacements at every 0.2 mm were defined, and three cycles per each target displacement were performed. In compression, absolute values for target loads equal to those reached in the corresponding half-cycles in tension were adopted until the achievement of the above mentioned limiting loads. Then, the target compressive load was kept constant in the subsequent cycles. For comparison, in cyclic tests B-50-12.9-CTO-50-1 and B-50-12.9-CTO-100-1 purely tensile loads were applied only.

In order to assess the influence of a preloading force on the connection behaviour in compression, preliminary tests in monotonic compression were carried out. A loading rate analogous to that used for monotonic pull-pull tests was adopted for these tests.

The load was supplied by an electromechanical actuator in displacement control and measured by a load cell with the nominal sensitivity of 2 mV/V. The longitudinal displacement of each connection was evaluated from measurements obtained by a couple of linear potentiometer sensors placed along two opposite faces of the specimen. Each sensor was connected, at one end, to the LVL member and, at the other end, to the outer hex nut, so that the gauge length was of 200 mm. Two more potentiometers with a gauge length of 420 mm were used to measure truss deformations in the intermediate part of the specimen and obtain estimates of the modulus of elasticity parallel to the grain. Finally, the overall stroke length was measured by means of two potentiometers connected with the grips of the loading apparatus, resulting in a total of 8 displacement sensors.

The adopted experimental setup is illustrated in Fig. 3a, whereas Fig. 3b shows one of the specimens at the beginning of test and the 8 displacement sensors. The arrangement and numbering of these sensors is shown in Fig. 4.

3. INFLUENCE OF PRELOADING FORCE ON COMPRESSION TESTS

The connection behaviour in compression is significantly influenced by the applied tightening torque. This is evident from Fig. 5, which compares the force-displacement responses obtained from three monotonic compression tests. In particular, curves 1 and 2 refer to specimens B-50-12.9-MCO-100-1 and B-50-12.9-MCO-100-2, respectively, tested in the absence of any tightening torque. In both tests, the compressive load, directly applied to the axial threaded rod at the specimen end, was transferred to the LVL member by means of the dowel-nut. Therefore, the area of the contact surface between timber section and dowel-nut was analogous to that occurring in tension tests, and the connection may be viewed as a steel-to-timber double shear connection (see Figs. 8.3f to h reported in [20]). The resulting failure mode showed a longitudinal splitting crack at both sides of the transverse hole which accommodates the dowel-nut (see Fig. 6a, b). Moreover, at the end of tests, the threaded rod showed an evident buckling shape (Fig. 6c). In fact, due to the rod-hole clearance, the threaded rod resulted to be weakly restrained against buckling.

Curve 3 in Fig. 5 refers to specimen B-50-12.9-MCO-100-3, whose dowel-nut connection was preliminarily tightened with a torque of 40 Nm. In this case the compressive load applied to the axial threaded rod was directly transferred to the LVL end section through the square washer. Then, the compression was resisted by the entire LVL bar and the connection stiffness showed a significant increase. Also the connection strength was increased compared with that exhibited by non-preloaded specimens. This was due to a change in the failure mode. In particular, for specimen B-50-12.9-MCO-100-3 the failure mode shown in Fig. 6, combining threaded rod instability with splitting in the LVL truss, completely disappeared. As a matter of fact, in the presence of tightened end connections, a compression member will attain global buckling combined with flexural failure. The aim of this research was to study the connection failure, rather than the strut buckling. Therefore, the specimens' length was reduced compared with typical lengths used in structures, so that strut buckling did not occur. The dashed part of the curve in Fig. 5 indicates that for an actual

structural element the compressive load may virtually be increased up to global buckling. Such an efficient response strictly depends on tightening, thanks to which the laterally unrestrained length of the threaded rod resulted dramatically reduced.

4. MONOTONIC PULL-PULL TESTS

Dowel-nuts made of class 12.9 threaded rods only were adopted for all of the monotonic tension tests. The main findings from these tests are summarized in the following separately for the three end distances a_1 = 50, 100 and 150 mm. The reader is referred to Table 2 for the whole matrix of experiments and results. The experimental force-displacement plots are reported in Fig. 7.

At the end of tests, no residual deformation was observed in the dowel-nut connectors. The failure modes described in the following paragraphs were then unaffected by interaction between LVL and steel connector deformabilities.

Due to the differences in preloading force adopted from test to test (Table 2), leading to a certain variability in the stiffnesses of the monotonic F-δ responses, considerations on mean value and scatter of displacement δ_{peak} corresponding to peak strength are believed to be not significant for MTO and MTP tests. Conversely, some comment on displacements will be reported in Sect. 5 with regard to cyclic tests, for which a unique value of the tightening torque was applied.

4.1. Case a_1 = 50 mm

For end distance a_1 = 50 mm (Fig. 7a, b) a linear elastic behaviour was observed up to the formation of a splitting crack in front of the dowel-nut (Fig. 8a). The corresponding failure load coincided with the peak capacity, F_{peak}, with the sole exception of specimen B-50-12.9-MTP-50-3 (curve 3 in Fig. 7a), for which a second, greater peak strength was encountered. For the other two specimens with the axis of the dowel-nut parallel to the veneer layers (curves 1 and 2 in Fig. 7a), a brittle collapse of the connection was observed following the achievement of F_{peak}. A second, but smaller peak strength was also obtained for all of the specimens with the axis of the dowel-nut orthogonal

to the veneer layers (Fig. 7b), which showed a relatively ductile behaviour with final displacements very larger than shown for parallel dowel-nut. These tests were interrupted when the extent of either displacement or strength degradation became so large to be considered not tolerable by real structures. Such behaviour was due to a stress reorganization following the splitting failure, leading the cracked specimens, after an initial strength degradation, to a stiffness recovery and a subsequent plug shear failure. Therefore, the final failure mode for these specimens corresponded to a plug shear mode superimposed to the initial splitting mode.

The mean value and CoV of F_{peak} for the specimens with the axis of the dowel-nut orthogonal to the veneer layers were 4% greater and 56% smaller, respectively, than for specimens with parallel dowel-nut. These percentages can be obtained from Table 3 using relation $100\times(x_O-x_P)/x_P$, where x_P and x_O indicate the generic quantity (mean value or CoV of F_{peak}) reported in the first and fourth table rows, respectively. It is worth noting that the preloading force influenced the slope of the initial linear elastic branch of the F-δ plot. In particular, the greater the applied tightening torque, the greater the initial stiffness was obtained. However, the preloading force did not influence the connection strength.

4.2. Case a_1 = 100 mm

For end distance a_1 = 100 mm (Fig. 7c, d), a significant increase in the connection strength was observed. In particular, for dowel-nut parallel and orthogonal to the veneer layers, the mean values of F_{peak} turned out to be 2.3 and 2.7 times, respectively, those obtained for a_1 = 50 mm (Table 3). Moreover, the mean value and CoV of F_{peak} for the specimens with dowel-nut axis orthogonal to the veneer layers were 24% greater and 64% smaller, respectively, than for specimens with parallel dowel-nut. Also the displacement corresponding to F_{peak} was influenced by the dowel-nut orientation, resulting, in the case of orthogonal dowel-nut, significantly greater than for parallel dowel-nut at equal tightening torque. For example, for specimens B-50-12.9-MTP-100-4 and B-50-12.9-MTO-100-1, for which a tightening torque of 80 Nm was applied, δ_{peak} resulted to be of 0.83

and 1.95 mm, respectively. Analogous considerations hold for tightening torques of 0 and 20 Nm (see tests No. 11, 12, 13, 16 and 17 in Table 2).

Specimens B-50-12.9-MTP-100-1 to B-50-12.9-MTP-100-4 failed in plug shear (Fig. 8b), whereas a splitting failure was observed for specimen B-50-12.9-MTO-100-1. For all of the other specimens with orthogonal dowel-nut, the failure mode was ruled by the coexistence of splitting and plug shear cracks in front of the dowel-nut. In any case, at the end of test, one or two longitudinal cracks were also evident behind the dowel-nut. These rear cracks formed due to the force exerted by the dowel-nut onto the faces of one front crack, which led to unbalanced transverse tensile stresses in front of the dowel-nut itself.

With regard to the elastic stiffness of the F-δ response, a strong influence of preload was observed. For example, adopting a tightening torque of 80 Nm (specimens B-50-12.9-MTO-100-1 and B-50-12.9-MTP-100-4) led to an angular coefficient of the regression line fitted to the F-δ response more than triple compared with that obtained for non-preloaded connections (see Figs. 7c, d and Table 2). Conversely, the preload effect on strength was not relevant.

4.3. Case a_1 = 150 mm

For end distance a_1 = 150 mm (Fig. 7e, f), an increase in ductility was observed for one of the specimens with the axis of the dowel-nut parallel to the veneer layers and for all of the specimens with orthogonal dowel-nut. Splitting was the prevailing failure mode for both parallel and orthogonal dowel-nut. A plug shear failure was observed for specimen B-50-12.9-MTP-150-2 only (Fig. 8c). A significantly smaller scatter of results in terms of F_{peak} was confirmed for orthogonal dowel-nut (Table 3). Compared with the case of a_1 = 100 mm, the mean value of F_{peak} for parallel and orthogonal dowel-nut was 3.9% greater and even 6.5% smaller, respectively. These findings indicate that, for the tested beech LVL, end distance $a_1 = 5d$ may be considered equivalent to the lower bound $a_1 = 7d$ prescribed in [20]. Future studies will be aimed at investigating the influence of edge distance a_2 orthogonal to the load direction.

Finally, the preload effects on the connection stiffness were analogous to those observed for a_1 = 100 mm (Table 2).

5. CICLYC PULL-PULL TESTS

Due to the loading protocol adopted (see Sect. 2.4), failure was always achieved in tension. All of the CO tests were begun in compression. The experimental force-displacement plots are reported in Figs. 9, 10 and 11 for end distance a_1 = 50, 100 and 150 mm, respectively. In each figure panel, the plots in the left column refer to specimens with dowel-nut obtained from class 12.9 threaded rods, whereas the right column plots are for connectors made of grade S355 steel.

5.1. Class 12.9 connector

For a_1 = 50 mm (Figs. 9a, c and e), in analogy with monotonic tests, a first and a subsequent peak strengths, corresponding to splitting and plug shear cracks, respectively, were encountered. The resulting failure mode is shown, for one of the specimens, in Fig. 8d. All of these tests were interrupted after the second peak strength for excess of either displacement or loss of resistance.

For a_1 = 100 mm, one only specimen failed in a mixed mode (Fig. 8e), whereas a plug shear failure was obtained for all of the others (Fig. 12a). Conversely, all of the specimens with a_1 = 150 mm failed in splitting (see Figs. 8f and 12b). In analogy with monotonic tests, no appreciable plastic deformation of the class 12.9 dowel-nut connector was attained.

The mean of the envelope curves of F-δ cyclic diagrams (restricted to tension only) is reported in red, for each end distance, in Figs. 7b, d and f. In particular, for a_1 = 100 mm (Figs. 7d), the slope gradient of the red curve within the elastic range substantially coincided with that obtained for monotonic test on specimen B-50-12.9-MTO-100-4. This specimen was initially preloaded with the same tightening torque (i.e., 40 Nm, see Table 2) as used for all of the cyclic tests. Therefore, a close correlation between preload and tensile stiffness of the connection was confirmed. For a_1 = 50 (Fig. 7b) and 150 mm (Fig. 7f), the mean stiffness showed in CO tests fitted that of monotonic curves for 20 Nm better than for 40 Nm. This feature was probably related with the cyclic loading

protocol adopted: beginning in compression may have led the connection to a preload reduction, so influencing the stiffness in the subsequent tension cycles.

Compared with MTO tests, the mean value of the load-carrying capacity obtained from cyclic tests was 11% smaller for $a_1 = 50$ mm, and 1% and 5% greater for $a_1 = 100$ and 150 mm, respectively. Therefore, load cycling did not cause any noticeable increase in strength degradation. Moreover, no particular influence on tension strength degradation appeared to be attributable to the previous cycles in compression. This is showed by comparison of Figs. 9e and 10g, referred to CTO tests for $a_1 = 50$ and 100 mm, respectively, with F-δ plots concerning CO tests for corresponding values of the end distance.

More significant differences occurred between monotonic and cyclic behaviour in terms of deformability in the damaged state. In particular, for $a_1 = 100$ mm, the mean value of δ_{peak} resulting from cyclic tests was 13% smaller than obtained from MTO tests (Table 3). Conversely, for $a_1 = 150$ mm, the mean of δ_{peak} for cyclic tests resulted 15% greater than for MTO tests. In terms of mean ultimate displacements δ_u, differences of cyclic with respect to MTO tests of −16% and +31% were found for $a_1 = 100$ and 150 mm, respectively.

5.2. Grade S355 connector

In cyclic tests on specimens with grade S355 dowel-nut connector, failure modes analogous to those obtained, at equal end distance, for class 12.9 connector were observed, with the exception of the case with $a_1 = 100$ mm. In particular, specimens with $a_1 = 50$ mm (Fig. 8g) failed in a splitting mode followed by a plug shear mode, and splitting was the prevailing failure mode for specimens with $a_1 = 150$ mm (Fig. 8i). For $a_1 = 100$ mm, the plug shear mode did not occur alone as shown in Fig. 12a, but always in combination with splitting cracks (see Fig. 8h). Moreover, at failure, the dowel-nut connector appeared undeformed for $a_1 = 50$ mm only (Fig. 8j), whereas it was affected by evident plastic deformations for $a_1 = 100$ (Fig. 8k) and 150 mm (Fig. 8l). For specimens B-50-

S355-CO-100-3 (Fig. 10f) and B-50-S355-CO-150-2 (Fig. 11d), the change in the slope gradient of the F-δ plot at about F = 25 kN was probably due to a premature loss of preload.

The dowel-nut connector grade did not affect, however, strength and deformability of the connection. Compared with cyclic tests described in Sect. 5.1, the mean value of F_{peak} resulted 10% greater for a_1 = 50 mm and 6% smaller for a_1 = 100 mm, whereas no appreciable difference was obtained for a_1 = 150 mm (see Table 3). Also the mean values of δ_{peak} agreed with those obtained for class 12.9 connector, particularly for end distances a_1 = 100 and 150 mm. Analogous remarks hold for ultimate displacements (Table 2).

The CoVs of F_{peak} did not exceed 12%. Excluding specimen B-50-S355-CO-150-2, for which a deformability significantly greater than that of the other specimens with a_1 = 150 mm was obtained, leads the CoVs of δ_{peak} not to exceed 19%.

6. DISCUSSION

Some comments on strength and stiffness of the tested connection and comparisons with consolidated design methods are reported in this Section.

6.1. Comparison with the Eurocode 5 design approach

The prevailing design approach for dowel-type connections is based on Johansen's yield theory [21], which assumes an ideally rigid-plastic behaviour of steel and timber (when subjected to embedment stresses). The load-carrying capacity is calculated by applying equilibrium conditions to different failure modes, which combine embedment failure in timber with bending deformations in the fasteners. Many current design codes, such as Eurocode 5 (EC5) [20], have adopted this approach. Additional design criteria are used to prevent premature failures, which are not covered by Johansen's theory. For example, requirements regarding spacing and end/edge distances of the fasteners, as well as reduction factors for connections with multiple fasteners in a row were introduced to prevent splitting along the grain and plug shear failure. Additionally, depending on

the type of fastener, a rope effect can be taken into account, provided that its contribution does not exceed a percentage of the load-carrying capacity according to Johansen's model (e.g., 25% for bolts, 0% for dowels). All these design rules have been developed primarily for softwood solid timber and glulam. For beech LVL, their validity still has to be verified.

In EC5 the characteristic value (index "k") of embedment strength f_h in case of predrilled holes is given as a linear function of dowel diameter d and characteristic value of wood density ρ_k:

$$f_{h,k} = 0.082(1 - 0.01d)\rho_k \,. \tag{1}$$

As observed above, with the only exception of specimens with grade S355 dowel-nut connector and $a_1 = 100$ or 150 mm (Figs. 8k, l), no plastic deformation of the dowel-nut took place in the experiments. Therefore, to estimate the characteristic value of the load-carrying capacity for the investigated connection the expression provided by EC5 for steel-to-timber double shear joints in the absence of fasteners yielding (see failure mode reported in Fig. 8.3f of [20]) was used. With regard to the connection comprised of a longitudinal threaded rod inserted into a hole of diameter d_0, and of a dowel-nut connector of diameter d and length l, this expression can be written in the following form:

$$F_{Rk} = f_{h,k}\left(dl - \pi d_0^2/4\right). \tag{2}$$

It is worth noting that in design codes the load-carrying capacity per fastener of any given connection is usually referred to one single shear plane. Conversely, for a more immediate comparison with the experimental results, Eq. (2) provides an estimate of the whole connection capacity.

Substituting the characteristic value of the LVL mass density provided by the manufacturer, $\rho_k = 680$ kg/m^3, into Eq. (1), and the resulting embedment strength ($f_{h,k} = 44.6$ MPa) into Eq. (2), yields $F_{Rk} = 38.7$ kN. If the mean wood density (index "m"), either that provided by the manufacturer, $\rho_m = 740$ kg/m^3, or that obtained from measurements on test specimens, $\rho_{m,meas} = 843$ kg/m^3 (Table 1), is used instead, an estimate of the mean load-carrying capacity is obtained. In

particular, for densities ρ_m and $\rho_{m,meas}$, the embedment strengths become $f_{h,m} = 48.5$ MPa and $f_{h,m,meas} = 55.3$ MPa, leading to capacities $F_{Rm} = 42.1$ kN and $F_{Rm,meas} = 48.0$ kN, respectively.

Table 3 reports, in percentage, the differences between predicted and experimental capacities. The former systematically underestimate the latter for end distances $a_1 = 100$ and 150 mm, with the better approximations being related with measured density $\rho_{m,meas}$ and MTP tests. For end distance $a_1 = 50$ mm, dramatically far away from standard-covered connections with $a_1/d \geq 7$, the experimental capacities are not negligible, being ranging between 41% and 47% of $F_{Rm,meas}$.

As an alternative to Eq. (1), the embedment strength may be calculated based on Eq. (2), but using experimental peak capacity, i.e.:

$$f_{h,peak} = F_{peak} / (dl - \pi d_0^2/4). \quad (3)$$

The strength values obtained from Eq. (3) are reported in Table 2 for each of the tests. With regard to cyclic and monotonic load tests for dowel-nut with the axis orthogonal to the veneer layers, $f_{h,peak}$ resulted to be ranging between 20 MPa and 28 MPa for $a_1 = 50$ mm, between 59 MPa and 75 MPa for $a_1 = 100$ mm and, finally, between 61 MPa and 77 MPa for $a_1 = 150$ mm.

In [18], the findings from monotonic embedment tests on a beech LVL having a maximum cross-layer percentage of 23% and measured average density of 765 kg/m^3 were presented. The influence of various parameters such as dowel diameter, spacing, end and edge distances was analyzed. In particular, 40 specimens were tested according to standard EN 383 [22], with a loaded end distance of 7d, whereas for other 30 specimens reduced end distances were adopted. It was shown that the presence of cross-layers allows reducing the end distances prescribed in [20]. Moreover, for $d = 20$ mm and end distance of 7d, the embedment strength resulted to be of 75 MPa at the threshold displacement of 5 mm and of 104 MPa at the peak capacity, corresponding to a displacement of 39 mm. Therefore, cross-layers prevent premature splitting failures, so enhancing both strength and displacement capacity of dowelled connections in beech LVL members. However, also the connections tested in this research, although lacking the beneficial effects due to

cross-layers, are believed to be adequate for structural applications, as it will be shown in future experimental studies.

6.2. Connection stiffness

For connections used in timber structures, the initial stiffness may be computed from the F-δ response as the secant stiffness either at 40% of the estimated peak capacity [23] or between $0.1F_{peak}$ and $0.4F_{peak}$ [24]. Some authors (see [25]) adopted the method recommended in [26] for the calculation of bending elastic modulus for timber members, based on a linear regression analysis of the F-δ response between $0.1F_{peak}$ and $0.4F_{peak}$.

Applying the first of the above mentioned methods to the non-preloaded specimens with a_1 = 100 and 150 mm, the corresponding mean stiffness would result to be $\overline{K}_{0.4}$ = 40.1 kN/mm. For comparison purposes, an estimate of the connection stiffness according to Table 7.1 of [20] may be also provided by the following expression:

$$K_{ser} = 2d\rho_{m,meas}^{1.5}/23, \quad (4)$$

where factor 2 indicates a double shear connection. Equation (4) yields stiffness K_{ser} = 42.6 kN/mm, which is in a very good agreement with $\overline{K}_{0.4}$.

For some of the connections tested in this research, the stiffening effects due to preload are only significant for very small values of the external tensile force. Therefore, in order to highlight the preload effects, the initial stiffnesses in tension were computed from fitting the various F-δ plots within intervals which do not necessarily comply with the standard's indication. To facilitate the comparison with the preloading force, initial tensile stiffness K_{j1} is reported in Table 2 for each specimen, together with the ends of the relevant regression interval expressed in percentage of F_{peak}.

Some experimental response in tension can be given, up to F_{peak}, a bilinear approximation. For these tests, also the secondary tensile stiffness, K_{j2}, is reported in Table 2 with the relevant regression interval.

For specimens tested in monotonic tension, the increase in K_{j1} with the applied tightening appears evident. For specimens tested under cyclic loading, a certain scatter in the K_{j1} values is observed, in spite of tightening torques invariably equal to 40 Nm. This scatter may be explained with the alternate application of tensile and compressive stresses, with compression being applied first, which led to uncontrolled preloading reductions. No particular trend of the stiffness with the end distance was observed, but this feature will deserve further analyses.

Based on the experimental results described, designers are discouraged to use non-preloaded connections in order to avoid excessive deformations under service loads.

CONCLUSIONS AND FUTURE DEVELOPMENTS

A total of 42 pull-pull tests and 3 monotonic compression tests on dowel-nut connector in LVL bar were carried out.

Non-preloaded connections tested in monotonic compression failed in splitting of the LVL bar combined with buckling of the longitudinal threaded rod. Conversely, preloading the connection with a tightening torque of 40 Nm led the compressive force to directly act on the whole end section of the LVL member. Therefore, a higher stiffness was observed in this case, and the test was stopped prior to failure.

The most significant results obtained from monotonic pull-pull tests can be summarized as follows.

- The connection stiffness appeared strongly influenced by preload. In particular, the greater the applied tightening torque, the greater the stiffness resulted to be. This would suggest using preload to control the connection deformation at failure.
- For the smallest end distance ($a_1/d = 2.5$), the mean capacity ($\overline{F}_{peak}$) resulted lying between 33% and 42% that obtained for $a_1/d = 7.5$. For $a_1/d = 5$, $\overline{F}_{peak}$ was almost the same as for $a_1/d = 7.5$.
- Compared with the case of connector having axis parallel to the veneer layers, aligning the dowel-nut axis orthogonally to the veneers led to an increase in $\overline{F}_{peak}$ of 24% and 11% for a_1/d

= 5 and 7.5, respectively. Correspondingly, a significant decrease in the coefficient of variation of F_{peak} (CoV_{Fpeak}) was observed. In particular, for $a_1/d = 5$, the CoV_{Fpeak} resulted equal to approximately 18% for parallel dowel-nut and 5% for orthogonal dowel-nut.

- The specimens with orthogonal dowel-nut showed, on average, a greater ductility than those with parallel dowel-nut, particularly for end distance $a_1 = 7.5d$. For these specimens a ratio between ultimate displacement (δ_u) and displacement at peak strength (δ_{peak}) lying in the range 1.14-1.45 was obtained. For specimens with end distance $a_1 = 2.5d$ the activation of a progressive failure mechanism led to an unexpectedly ductile response. Conversely, a substantially elastic-brittle behaviour was obtained for specimens with $a_1 = 5d$, with a mean displacement at failure of about 2 mm.

With regard to cyclic tests, the following conclusions can be drawn.

- Due to the use of one only value of the tightening torque, the elastic stiffnesses resulted significantly less scattered than those obtained from monotonic tests.
- Compared with monotonic pull-pull tests on specimens with orthogonal dowel-nut, the mean value of F_{peak} from cyclic tests on class 12.9 connector resulted to be 13% smaller for $a_1 = 2.5d$, but substantially coincident for both $a_1 = 5d$ and $7.5d$, indicating that the application of alternate tensile and compressive loads did not cause any noticeable increase in strength degradation.
- The use of grade S355 steel involved, at failure, evident plastic deformations of the connector for end distances $a_1 = 5d$ and $7.5d$. However, the smaller connector yield strength did not affect strength and overall deformability of the connection, which agree with those obtained for class 12.9 dowel-nut.

Finally, on-the-safe-side estimates of the load-carrying capacity of the connection were provided based on Johansen's theory (see Eqs. (1) and (2)). As expected, the better prediction was obtained making use of the mean value of mass density measurements from 8 test specimens.

This study was aimed at exploring failure modes involving timber collapse only. For this reason, class 12.9 longitudinal threaded rods were used. During the tests, these rods did not ever reach their yield strength. Based on the load-carrying capacities obtained, the use of class 8.8 threaded rods would involve, for $a_1 \geq 5d$, rod plastic deformations (and rupture in some case), and then a significant increase in ductility. Enhanced ductility could also be achieved using either a LVL with a certain amount of cross-layers [18] or dowels with optimized post-elastic properties [27].

As a matter of fact, the tested connection proved to be suitable for use in truss structures where design is mainly controlled by strength, rather than by ductility and energy dissipation capacity. The adopted beech LVL ensures very high mechanical performance, which allows limiting cross-section dimensions of bars, but may be somewhat difficult to exploit. Future studies will then be devoted to the experimental analysis of analogous connections in LVL bars of different cross-sections and wood species, as well as of prototypes of spatial LVL bar assemblages.

The interested reader is referred to the whole set of experimental results from pull-pull tests, which is provided as supplementary material attached to this paper.

ACKNOWLEDGMENTS

The present investigation was developed in the framework of the industrial innovation project TIRISICO (PG/2015/737636) granted by Regione Emilia-Romagna, POR-FESR 2014-2020 (Region Operational Program for the European Regional Development Fund). LVL made of European beech was produced by Pollmeier GmbH & Co. KG. The test specimens were supplied by Pradelli srl in Modena, Italy. A special acknowledgement is due to Drs. Massimo Cont, Fabio Dall'Aglio and Massimo Pradelli for their contribution to the preparation of the test specimens. The contribution of Mr. Roberto Mazza to the preparation of some experiments is also acknowledged.

REFERENCES

[1] M. Nale, F. Minghini, A. Chiozzi, A. Tralli, Fragility functions for local failure mechanisms in unreinforced masonry buildings: a typological study in Ferrara, Italy. Bull. Earthq. Eng. (2021). DOI: https://doi.org/10.1007/s10518-021-01199-6.

[2] N. Tullini, F. Minghini, Cyclic test on a precast reinforced concrete column-to-foundation grouted duct connection. Bull. Earthq. Eng. 18(4) (2020) 1657–1691.

[3] F. Minghini, F. Lippi, W. Salvatore, N. Tullini, Pullout tests on the connection to an existing foundation of a steel warehouse rebuilt after the 2012 Emilia (Italy) earthquakes. Bull. Earthq. Eng. 19(11) (2021) 4369–4405.

[4] F. Minghini, N. Tullini, Seismic retrofitting solutions for precast RC industrial buildings struck by the 2012 earthquakes in Norther Italy 2012. Front. Built Environ. 7 (2021) 631315.

[5] A. Bukauskas, P. Mayencourt, P. Shepherd, B. Sharma, C. Mueller, P. Walker, J. Bregulla, Whole timber construction: A state of the art review. Constr. Build. Mater. 213 (2019) 748–769.

[6] A. Brose, Peripheral timber: applications for waste wood material in extreme climates and earthquake risk regions, Massachusetts Institute of Technology, Cambridge, Massachusetts, Master's thesis, 2018. https://dspace.mit.edu/handle/1721.1/122902.

[7] G. Quaranta, C. Demartino, Y. Xiao, Experimental dynamic characterization of a new composite glubam-steel truss structure. Journal of Building Engineering 25 (2019) 100773.

[8] C.A. Eckelman, Strength of furniture joints constructed with through-bolts and dowel-nuts, Forest Prod. J. 39(11/12) (1989) 41–48.

[9] C.A. Eckelman, Textbook of product engineering and strength design of furniture, Purdue University Press, West Lafayette, Indiana, 2003.

[10] C.A. Eckelman, Withdrawal and bending strength of dowel-nuts in plywood and oriented strand board, Forest Prod. J. 53(6) (2003) 54–57.

[11] C.A. Eckelman, J.F. Senft, Truss system for developing countries using small diameter roundwood and dowel nut construction. Forest Prod. J. 45(10) (1995) 77–80.

[12] R.W. Wolfe, J.R. King, A. Gjinolli, Dowel-nut connection in Douglas-fir peeler cores, Research Paper FPL-RP-586, U.S. Department of Agriculture, Forest Service, Forest Products Laboratory, Madison, Wisconsin, 2000.

[13] T.F.M. Morgado, A.M.P.G. Dias, J.S. Machado, J.H. Negrão, Structural connections for small-diameter poles, J. Struct. Eng. 139(11) (2013) 2003–2009.

[14] Bundesamt für Umwelt, Jahrbuch Wald und Holz - Annuaire La forêt et le bois, Bundesamt für Umwelt BAFU, Bern, 2020.

[15] M. Knorz, J.-W. van de Kuilen, Development of a high-capacity engineered wood product – LVL made of European Beech (fagus sylvatica L.), in: P. Quenneville (Ed.), Proc. of the 12th World Conference of Timber Engineering (WCTE 2012), Auckland, New Zealand, 2012, pp. 487–497.

[16] G. Dill-Langer, S. Aicher, Glulam composed of glued laminated veneer lumber made of beech wood: superior performance in compression loading, in: S. Aicher, H.W. Reinhardt, H. Garrecht (Eds.), Materials and Joints in Timber Structures, Springer, Netherlands, 2014, pp. 603–613.

[17] P. Kobel, R. Steiger, A. Frangi, Experimental analysis on the structural behaviour of connections with LVL made of beech wood, in: S. Aicher, H.W. Reinhardt, H. Garrecht (Eds.), Materials and Joints in Timber Structures, Springer, Netherlands, 2014, pp. 211–220.

[18] P. Kobel, A. Frangi, R. Steiger, R. Steiger, Dowel-type connections in LVL made of beech wood, in Proceedings of the first International Network on Timber Engineering Research (INTER), Bath, United Kingdom, 2014, pp. 103–115.

[19] P. Kobel, A. Frangi, R. Steiger, Timber trusses made of European beech LVL, in: J. Eberhardsteiner, W. Winter, A. Fadai, M. Pöll (Eds.), Proc. of the 14th World Conference on Timber Engineering (WCTE 2016), Wien, Austria, 2016, pp. 635–642.

[20] EN 1995-1-1:2010-12. Eurocode 5: Design of timber structures - Part 1-1: General – Common rules and rules for buildings.

[21] K. Johansen, Theory of Timber Connections. International Association for Bridge and Structural Engineering Publications 9 (1949) 249–262.

[22] EN 383:2007. Timber Structures - Test methods - Determination of embedment strength and foundation values for dowel type fasteners.

[23] EN 26891:1991. Timber structures - Joints made with mechanical fasteners - General principles for the determination of strength and deformation characteristics.

[24] EN 12512:2001. Timber structures - Test methods - Cyclic testing of joints made with mechanical fasteners.

[25] J. Gamerro, J.F. Bocquet, Y. Weinand, A calculation method for interconnected timber elements using wood-wood connections. Buildings 10(3) 61 (2020). DOI: https://doi.org/10.3390/buildings10030061.

[26] EN 408:2010. Timber structures - Structural timber and glued laminated timber - Determination of some physical and mechanical properties.

[27] M. Geiser, M. Bergmann, M. Follesa, Influence of steel properties on the ductility of doweled timber connections. Construction and Building Materials 266 (2021) 121152.

FIGURE CAPTIONS

Fig. 1. Axonometric cross-section of the threaded rod with dowel-nut connector in a LVL member.

Fig. 2. Execution phases of the threaded rod with dowel-nut connector.

Fig. 3. Experimental setup: (a) schematic of the test rig and (b) view of one of the specimens at the beginning of test.

Fig. 4. Arrangement of linear potentiometers used for displacement measurements.

Fig. 5. Force-displacement responses obtained from tests in monotonic compression (MCO tests). Curves 1 and 2: specimens B-50-12.9-MCO-100-1 and B-50-12.9-MCO-100-2 with no preloading force; curve 3: specimen B-50-12.9-MCO-100-3 with preload corresponding to a tightening torque of 40 Nm.

Fig. 6. Non-preloaded specimens at the end of MTO tests: (a, b) splitting failure of the LVL member due to compressive stresses exerted by the dowel-nut and (c) buckling of the threaded rod.

Fig. 7. Force-displacement responses obtained from tests in monotonic tension: (a, c, e) MTP and (b, d, f) MTO tests. Longitudinal edge distance (a, b) a_1 = 50 mm, (c, d) 100 mm and (e, f) 150 mm. Curve labels in the subplots correspond to the numbers at the end of specimens' labels reported in the second column of Table 2. Red curves in (b, d, f) are the (tension parts of the) mean envelope diagrams obtained from cyclic pull-pull tests on specimens with class 12.9 dowel-nut connector.

Fig. 8. Tensile failure of beech LVL specimens with dowel-nut connector: observed collapse modes (a, b, c) in monotonic tension (MTP), and after cyclic tests on (d, e, f) class 12.9 and (g, h, i) grade S355 dowel-nuts. (j, k, l) grade S355 connectors at the end of cyclic tests. Longitudinal edge distance (a, d, g, j) a_1 = 50 mm, (b, e, h, k) 100 mm and (c, f, i, l) 150 mm.

Fig. 9. Force-displacement diagrams obtained from cyclic tests on specimens with dowel-nut at edge distance a_1 = 50 mm: connectors made of (a, c, e) class 12.9 and (b, d, f) grade S355 steel.

Fig. 10. Force-displacement diagrams obtained from cyclic tests on specimens with dowel-nut at edge distance a_1 = 100 mm: connectors made of (a, c, e) class 12.9 and (b, d, f) grade S355 steel.

Fig. 11. Force-displacement diagrams obtained from cyclic tests on specimens with dowel-nut at edge distance a_1 = 150 mm: connectors made of (a, c, e) class 12.9 and (b, d, f) grade S355 steel.

Fig. 12. Failure modes observed at the end of cyclic pull-pull tests (class 12.9 connectors): (a) specimen B-50-12.9-CO-100-1; (b) specimen B-50-12.9-CO-150-2.

TABLE CAPTIONS

Table 1. Material and mechanical properties of beech LVL based on measured and manufacturer's data. Tests were conducted in accordance with [26].

Table 2. Matrix of experimental tests reporting, for each specimen, measured capacity F_{peak} and corresponding embedment strength f_h and displacement δ_{peak}, ultimate displacement δ_u and failure mode. Also reported in the table are the initially applied tightening torques and stiffnesses of the F-δ plots with the relevant computation intervals.

Table 3. Mean values and coefficient of variations of F_{peak} ($\overline{F}_{peak}$, CoV_{Fpeak}) and δ_{peak} ($\overline{\delta}_{peak}$, $CoV_{\delta peak}$) for homogeneous series of test specimens. Also reported in the table are the percent differences ($Diff_1$, $Diff_2$ and $Diff_3$) between experimental and predicted capacities.

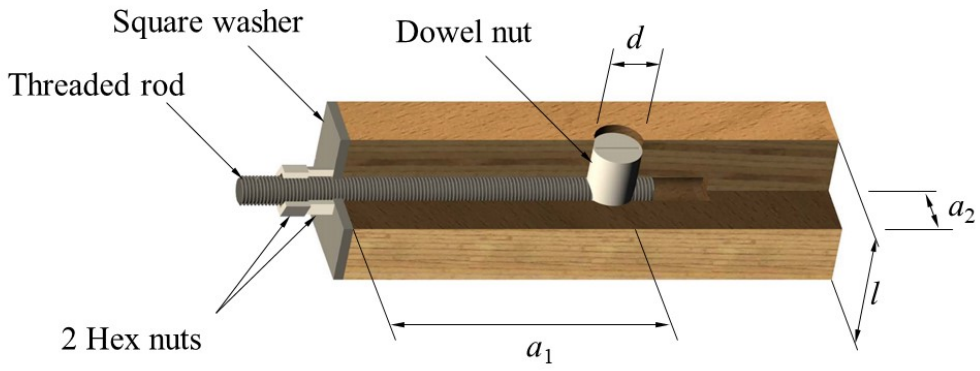

Fig. 1. Axonometric cross-section of the threaded rod with dowel-nut connector in a LVL member.

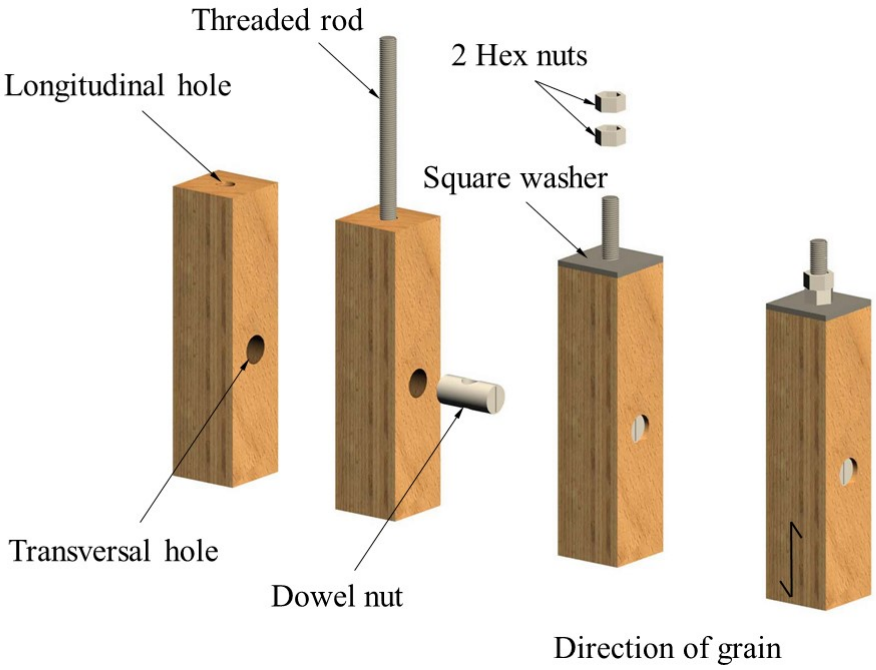

Fig. 2. Execution phases of the threaded rod with dowel-nut connector.

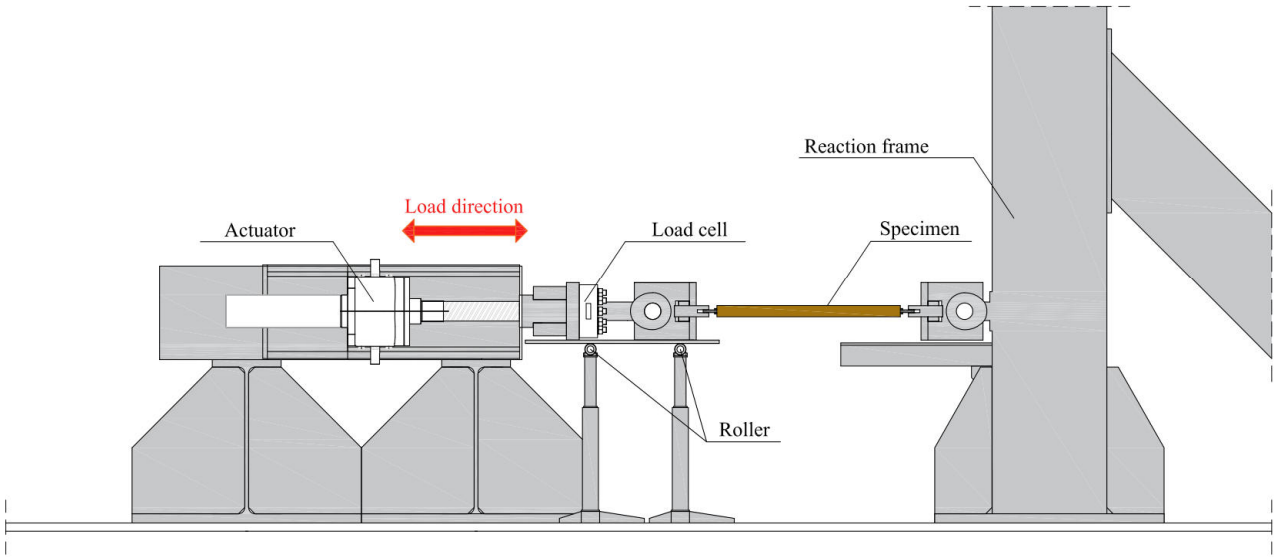

(a)

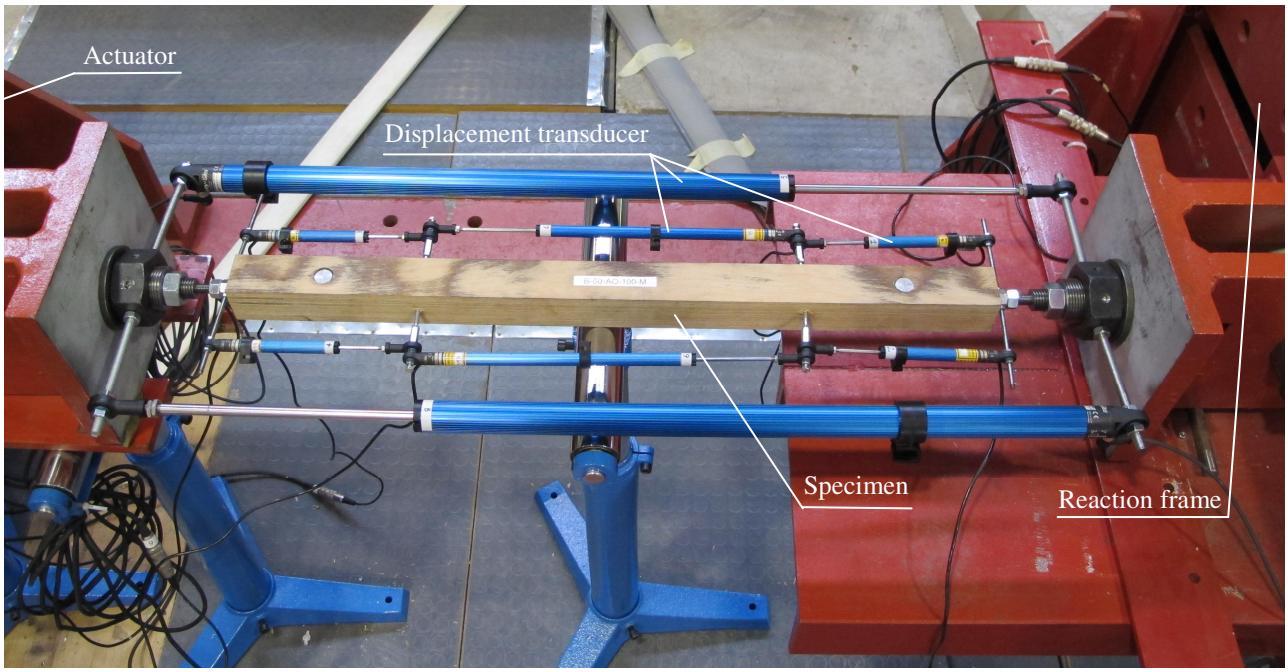

(b)

Fig. 3. Experimental setup: (a) schematic of the test rig and (b) view of one of the specimens at the beginning of test.

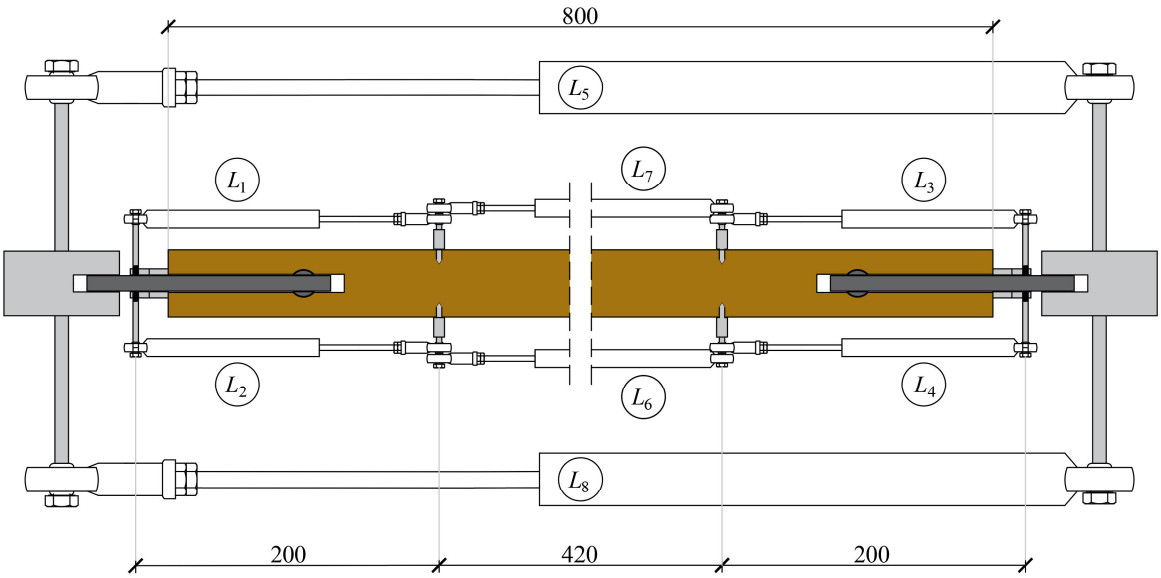

Fig. 4. Arrangement of linear potentiometers used for displacement measurements.

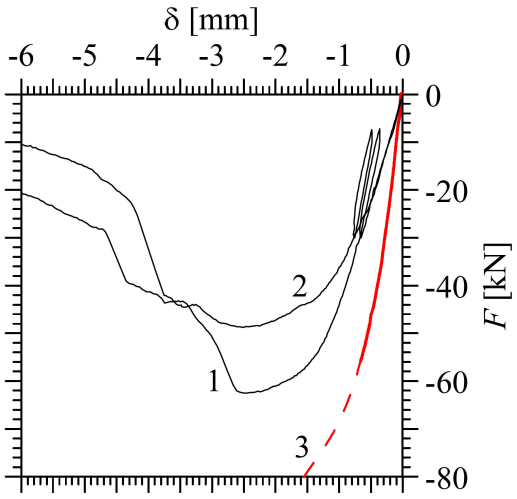

Fig. 5. Force-displacement responses obtained from tests in monotonic compression (MCO tests). Curves 1 and 2: specimens B-50-12.9-MCO-100-1 and B-50-12.9-MCO-100-2 with no preloading force; curve 3: specimen B-50-12.9-MCO-100-3 with preload corresponding to a tightening torque of 40 Nm.

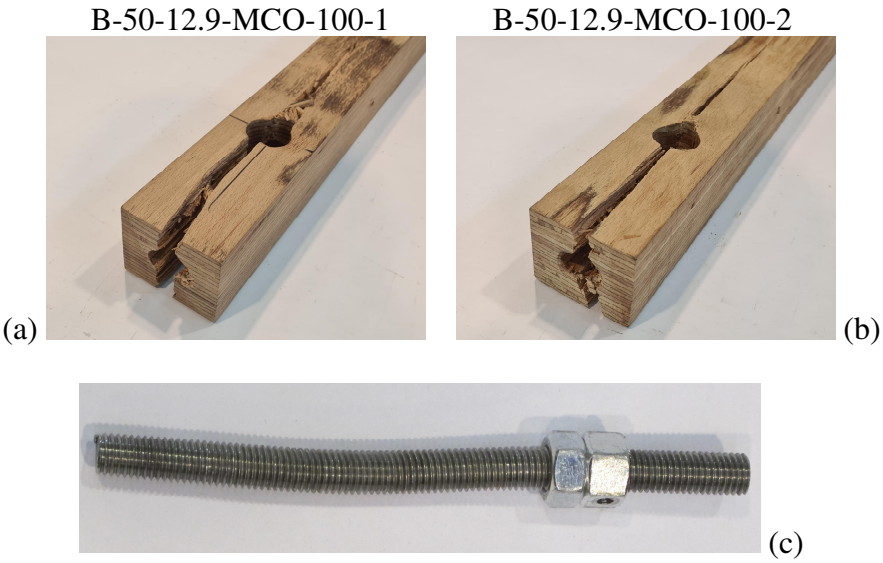

Fig. 6. Non-preloaded specimens at the end of MTO tests: (a, b) splitting failure of the LVL member due to compressive stresses exerted by the dowel-nut and (c) buckling of the threaded rod.

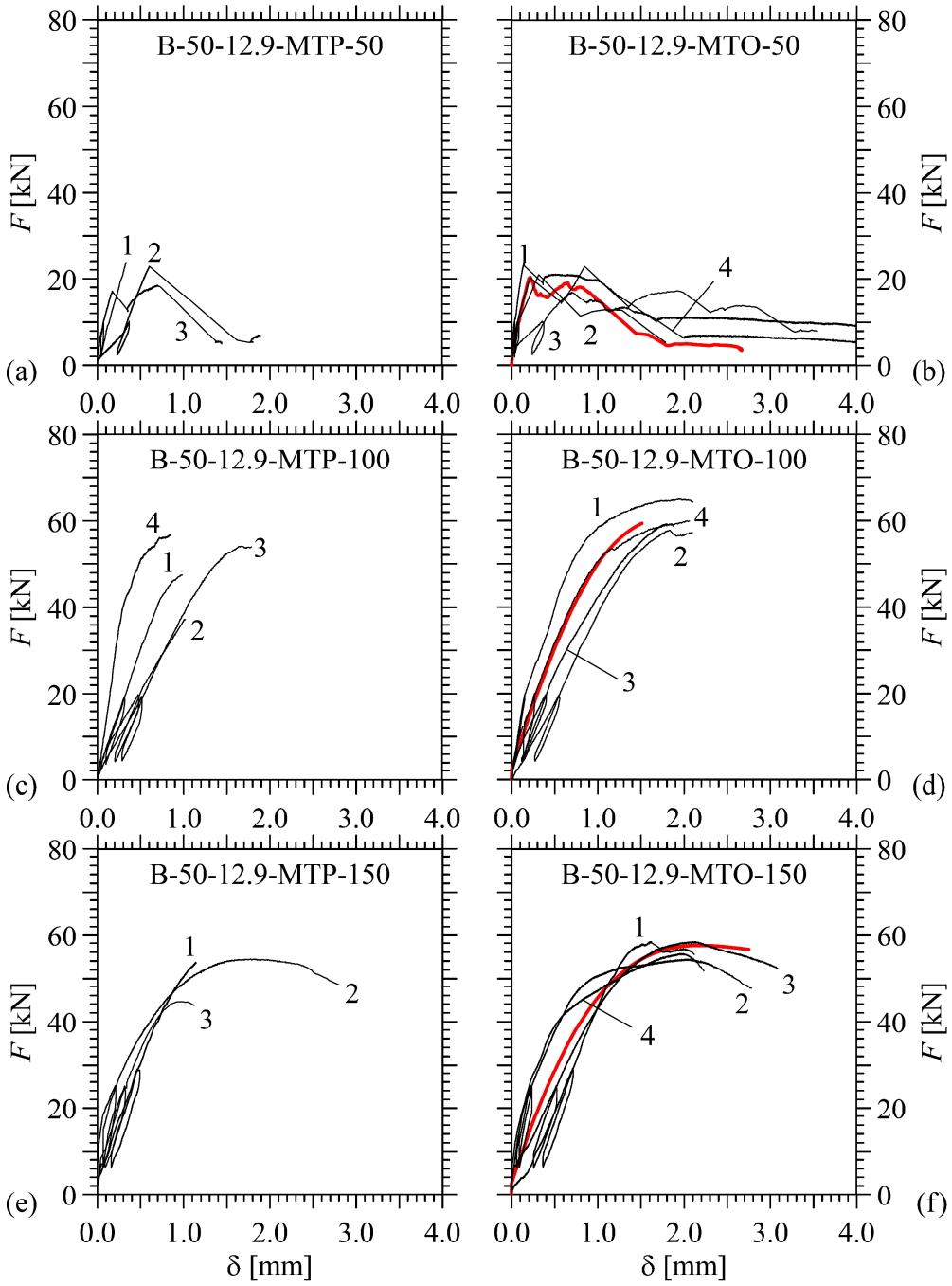

Fig. 7. Force-displacement responses obtained from tests in monotonic tension: (a, c, e) MTP and (b, d, f) MTO tests. Longitudinal edge distance (a, b) a_1 = 50 mm, (c, d) 100 mm and (e, f) 150 mm. Curve labels in the subplots correspond to the numbers at the end of specimens' labels reported in the second column of Table 2. Red curves in (b, d, f) are the (tension parts of the) mean envelope diagrams obtained from cyclic pull-pull tests on specimens with class 12.9 dowel-nut connector.

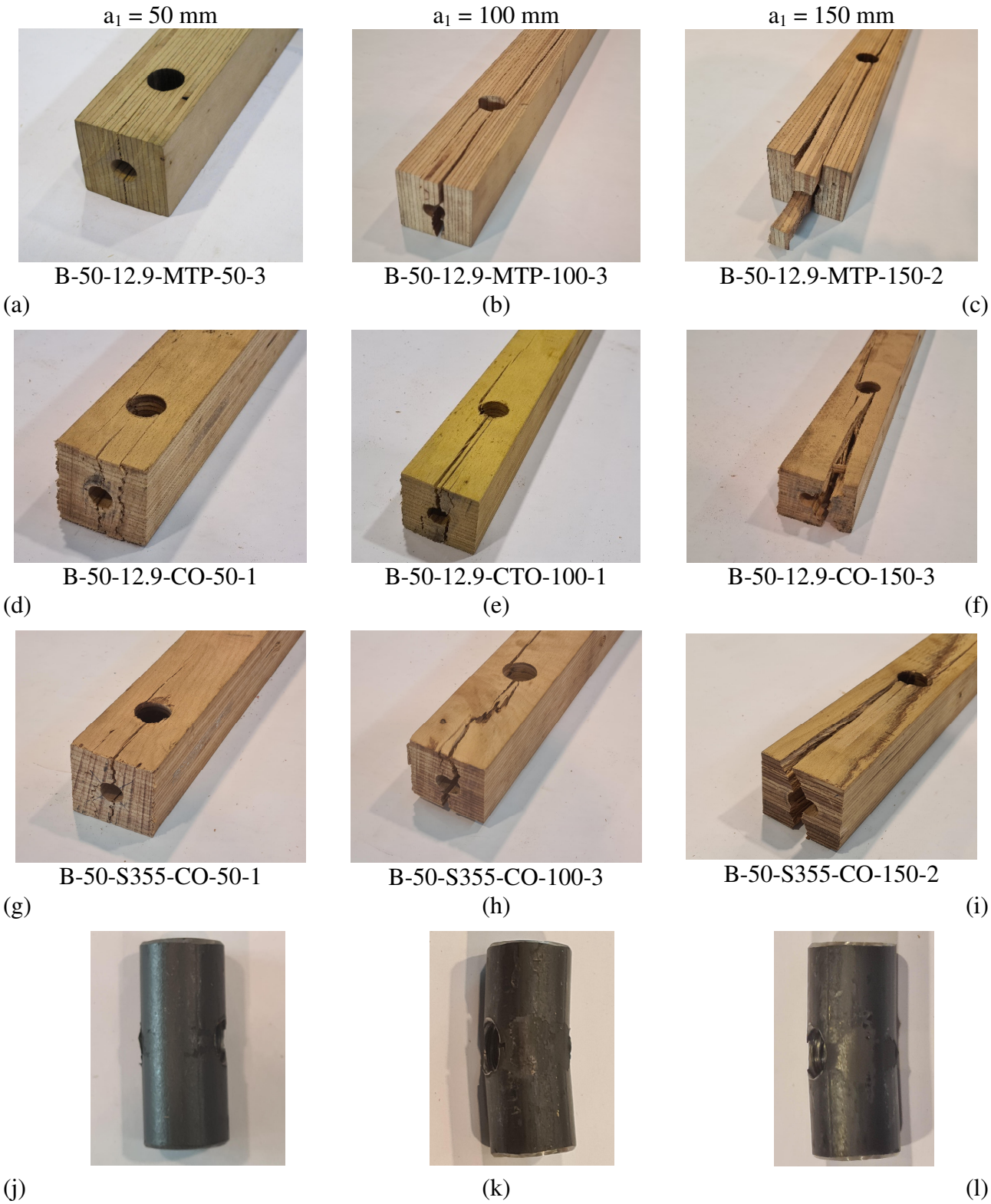

Fig. 8. Tensile failure of beech LVL specimens with dowel-nut connector: observed collapse modes (a, b, c) in monotonic tension (MTP), and after cyclic tests on (d, e, f) class 12.9 and (g, h, i) grade S355 dowel-nuts. (j, k, l) grade S355 connectors at the end of cyclic tests. Longitudinal edge distance (a, d, g, j) a_1 = 50 mm, (b, e, h, k) 100 mm and (c, f, i, l) 150 mm.

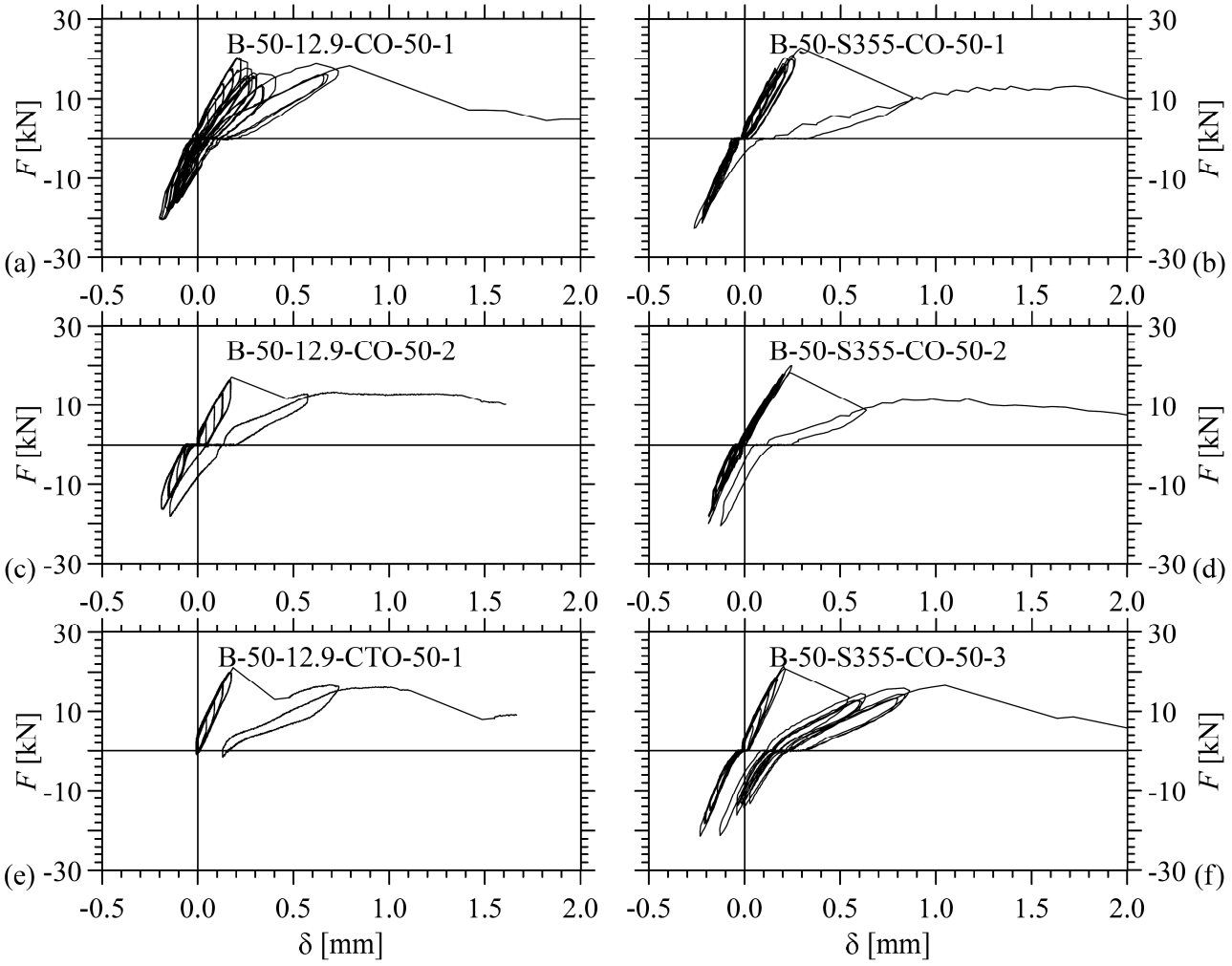

Fig. 9. Force-displacement diagrams obtained from cyclic tests on specimens with dowel-nut at edge distance a_1 = 50 mm: connectors made of (a, c, e) class 12.9 and (b, d, f) grade S355 steel.

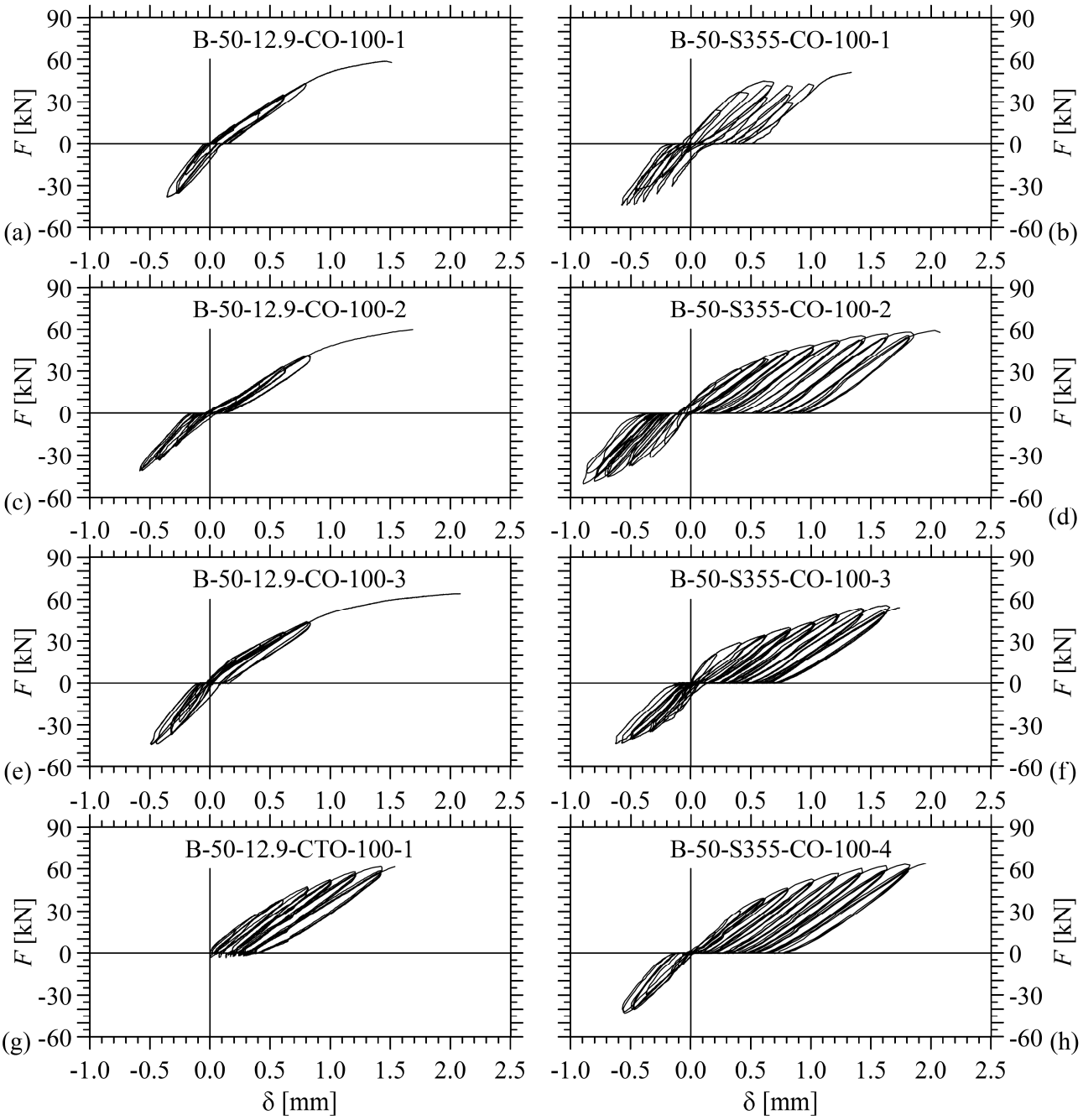

Fig. 10. Force-displacement diagrams obtained from cyclic tests on specimens with dowel-nut at edge distance a_1 = 100 mm: connectors made of (a, c, e) class 12.9 and (b, d, f) grade S355 steel.

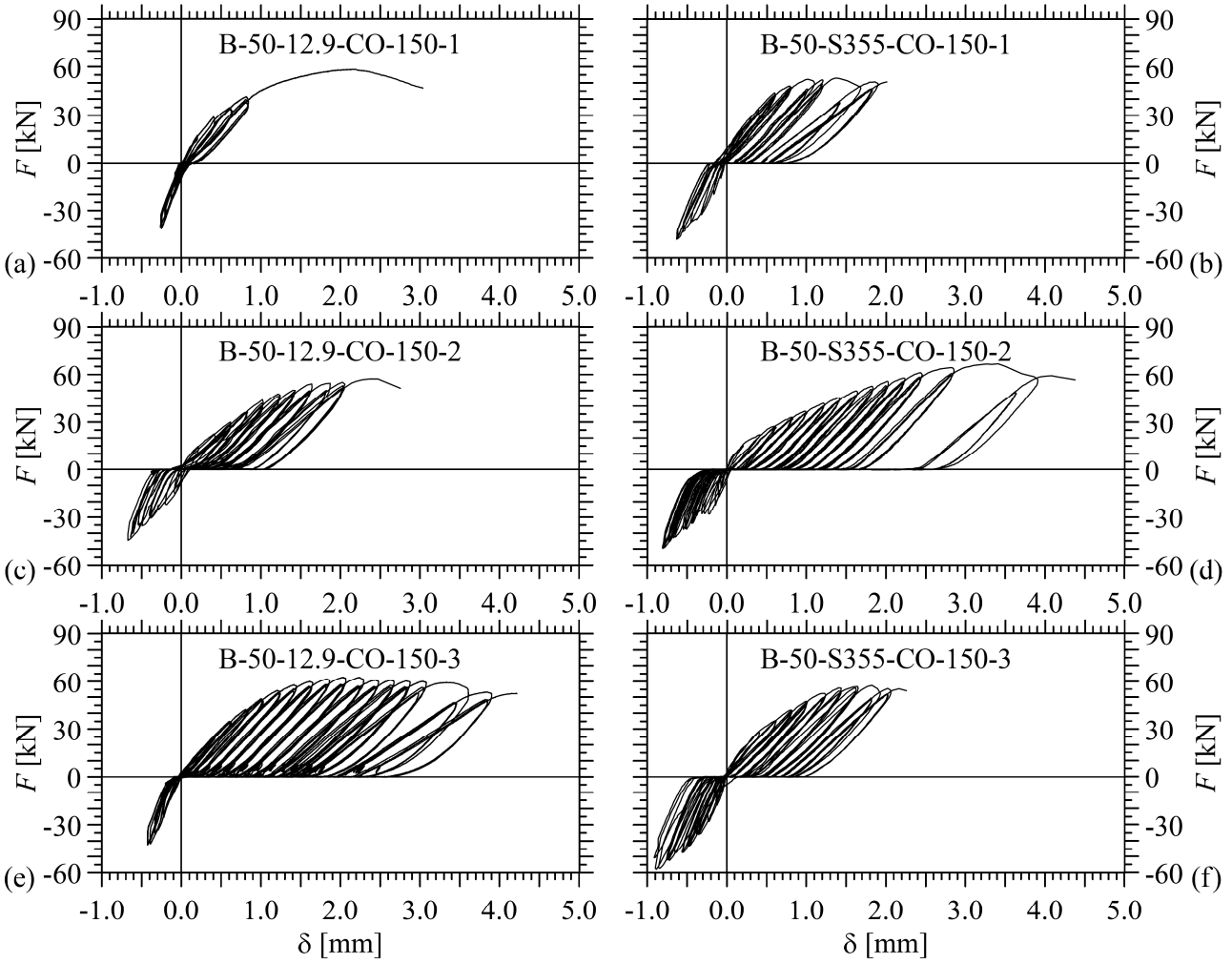

Fig. 11. Force-displacement diagrams obtained from cyclic tests on specimens with dowel-nut at edge distance a_1 = 150 mm: connectors made of (a, c, e) class 12.9 and (b, d, f) grade S355 steel.

(a) (b)

Fig. 12. Failure modes observed at the end of cyclic pull-pull tests (class 12.9 connectors): (a) specimen B-50-12.9-CO-100-1; (b) specimen B-50-12.9-CO-150-2.

Table 1. Material and mechanical properties of beech LVL based on measured and manufacturer's data. Tests were conducted in accordance with [26].

Selected properties	**Symbol**	**Measured data**		**Manufacturer's data**
		Number of specimens	Test results (CoV)	
Mass density [kg/m^3]	ρ_m	8	843 (2.5%)	≥ 740
	ρ_k			≥ 680
Flatwise bending strength [MPa]	f_m	3	112 (3.3%)	
	$f_{m,k}$			$(600/50)^{0.14} \times 70 = 99$
Compressive strength parallel to the grain [MPa]	$f_{c,0,m}$	8	95 (2.4%)	
	$f_{c,0,k}$			59.4
Modulus of elasticity parallel to the grain [GPa]	$E_{t,0,m}$	17	16.6 (15.8%)	16.7
Moisture Content [%]	MC	17	7.4 (5.0%)	5-10

Table 2. Matrix of experimental tests reporting, for each specimen, measured capacity F_{peak} and corresponding embedment strength f_h and displacement δ_{peak}, ultimate displacement δ_u and failure mode. Also reported in the table are the initially applied tightening torques and stiffnesses of the F-δ plots with the relevant computation intervals.

Test #	Specimen label	End distance [mm]	Dowel-nut grade	Dowel-nut orientation	Loading protocol	Peak capacity [kN]	Embedment strength [MPa]	Displacement at F_{peak} [mm]	Ultimate displacement [mm]	Failure mode[(b)]	Tightening torque [Nm]	Initial stiffness [kN/mm]	F/F_{peak} range for K_{j1} [%]-[%]	Secondary stiffness [kN/mm]	F/F_{peak} range for K_{j2} [%]-[%]
	Symbols	a_1				F_{peak}	$f_{h,peak}$	δ_{peak}	δ_u[(a)]		M_t	K_{j1}		K_{j2}	
1	B-50-12.9-MTP-50-1	50	12.9	P	M	23.8	27.4	0.33	Int.	II	20	95	15-35		
2	B-50-12.9-MTP-50-2	50	12.9	P	M	22.9	26.3	0.60	Int.	II	0	20	10-30		
3	B-50-12.9-MTP-50-3	50	12.9	P	M	17.0	19.6	0.17	Int.	III	40	140	10-40	70	60-80
4	B-50-12.9-MTO-50-1	50	12.9	O	M	23.9	27.5	0.15	Int.	III	40	190	20-40	150	40-80
5	B-50-12.9-MTO-50-2	50	12.9	O	M	21.2	24.4	0.32	Int.	III	20	115	15-35		
6	B-50-12.9-MTO-50-3	50	12.9	O	M	22.9	26.4	0.85	Int.	III	0	20	20-35		
7	B-50-12.9-MTO-50-4	50	12.9	O	M	20.3	23.4	0.22	Int.	III	40	150	15-40		
8	B-50-12.9-CO-50-1	50	12.9	O	C	20.5	23.7	0.21	Int.	III	40	100	10-40		
9	B-50-12.9-CO-50-2	50	12.9	O	C	17.1	19.7	0.18	Int.	III	40	130	10-40	90	50-70
10	B-50-12.9-CTO-50-1	50	12.9	O	CT[(c)]	21.1	24.4	0.19	Int.	III	40	105	20-40		
11	B-50-12.9-MTP-100-1	100	12.9	P	M	47.7	55.0	0.98	0.99	II	20	60	10-40		
12	B-50-12.9-MTP-100-2	100	12.9	P	M	37.4	43.1	1.02	1.03	II	0	40	15-40		
13	B-50-12.9-MTP-100-3	100	12.9	P	M	54.4	62.7	1.68	1.79	II	0	40	10-40		
14	B-50-12.9-MTP-100-4	100	12.9	P	M	56.9	65.5	0.83	0.83	II	80	140	10-40		
15	B-50-12.9-MTO-100-1	100	12.9	O	M	65.1	75.1	1.95	2.12	I	80	130	5-30	55	30-50
16	B-50-12.9-MTO-100-2	100	12.9	O	M	58.0	66.8	1.83	2.10	IV	0	40	10-40		
17	B-50-12.9-MTO-100-3	100	12.9	O	M	59.3	68.4	1.79	1.88	IV	20	60	5-15	40	15-40
18	B-50-12.9-MTO-100-4	100	12.9	O	M	60.1	69.3	2.07	2.07	IV	40	115	3-10	55	15-50
19	B-50-12.9-CO-100-1	100	12.9	O	C	58.7	67.7	1.45	1.51	II	40	55	10-30		
20	B-50-12.9-CO-100-2	100	12.9	O	C	59.8	68.9	1.69	1.70	II	40	60	20-40		
21	B-50-12.9-CO-100-3	100	12.9	O	C	64.0	73.8	2.06	2.08	II	40	75	10-30	40	30-60
22	B-50-12.9-CTO-100-1	100	12.9	O	CT[(c)]	61.7	71.1	1.42	1.54	IV	40	65	10-40		
23	B-50-12.9-MTP-150-1	150	12.9	P	M	53.7	61.9	1.14	1.14	I	20	60	10-40		
24	B-50-12.9-MTP-150-2	150	12.9	P	M	54.5	62.8	1.86	2.80	II	80	450	10-20	145	20-30
25	B-50-12.9-MTP-150-3	150	12.9	P	M	44.7	51.6	0.93	1.15	I	40	125	2-13	75	20-45
26	B-50-12.9-MTO-150-1	150	12.9	O	M	58.3	67.3	1.61	2.12	I	0	45	10-40		
27	B-50-12.9-MTO-150-2	150	12.9	O	M	54.4	62.7	2.02	2.78	I	80	150	5-25	115	25-35
28	B-50-12.9-MTO-150-3	150	12.9	O	M	58.4	67.3	2.12	3.08	I	20	100	7-10	40	15-40
29	B-50-12.9-MTO-150-4	150	12.9	O	M	55.6	64.2	1.95	2.23	I	40	150	10-20	80	20-40
30	B-50-12.9-CO-150-1	150	12.9	O	C	58.4	67.4	2.18	3.04	I	40	95	10-30		
31	B-50-12.9-CO-150-2	150	12.9	O	C	57.5	66.3	2.41	2.75	I	40	65	10-20	40	20-40
32	B-50-12.9-CO-150-3	150	12.9	O	C	62.7	72.3	2.03	4.22	I	40	55	10-40		
33	B-50-S355-CO-50-1	50	S355	O	C	22.8	26.3	0.29	Int.	III	40	105	10-35		
34	B-50-S355-CO-50-2	50	S355	O	C	20.3	23.4	0.25	Int.	III	40	85	10-40		
35	B-50-S355-CO-50-3	50	S355	O	C	21.6	24.9	0.20	Int.	III	40	109	10-40		
36	B-50-S355-CO-100-1	100	S355	O	C	50.7	58.5	1.33	1.34	IV	40	105	10-40		
37	B-50-S355-CO-100-2	100	S355	O	C	59.2	68.3	2.03	2.08	IV	40	90	10-30		
38	B-50-S355-CO-100-3	100	S355	O	C	55.7	64.2	1.62	1.74	IV	40	100	10-30		
39	B-50-S355-CO-100-4	100	S355	O	C	64.1	73.9	1.97	1.97	IV	40	80	10-40		
40	B-50-S355-CO-150-1	150	S355	O	C	53.2	61.3	1.39	2.01	IV	40	90	10-30		
41	B-50-S355-CO-150-2	150	S355	O	C	66.7	76.9	3.36	4.44	I	40	55	10-30	25	30-60
42	B-50-S355-CO-150-3	150	S355	O	C	57.6	66.4	1.82	2.26	I	40	115	10-15	50	20-40

(a) Int. = test interrupted for excess of displacement or strength loss;

(b) Observed failure modes were: I = splitting; II = plug shear; III = splitting followed by plug shear; and IV = simultaneous splitting and plug shear;

(c) CT = cyclic loading in tension only.

Table 3. Mean values and coefficient of variations of F_{peak} ($\overline{F}_{peak}$, CoV_{Fpeak}) and δ_{peak} ($\overline{\delta}_{peak}$, $CoV_{\delta peak}$) for homogeneous series of test specimens. Also reported in the table are the percent differences ($Diff_1$, $Diff_2$ and $Diff_3$) between experimental and predicted capacities.

Specimen series	Test #	Peak capacity					Displacement at F_{peak}	
		$\overline{F}_{peak}$	CoV_{Fpeak}	$Diff_1$ [b]	$Diff_2$ [c]	$Diff_3$ [d]	$\overline{\delta}_{peak}$	$CoV_{\delta peak}$
		[kN]	[%]	[%]	[%]	[%]	[mm]	[%]
B-50-12.9-MTP-50[a]	1, 2, 3	21.2	17.4	82.5	98.5	126.2		
B-50-12.9-MTP-100	11, 12, 13, 14	49.1	17.7	-21.1	-14.2	-2.2	1.12	33.4
B-50-12.9-MTP-150	23, 24, 25	51.0	10.6	-24.1	-17.4	-5.9	1.31	37.1
B-50-12.9-MTO-50[a]	4, 5, 6, 7	22.1	7.3	75.4	90.9	117.4		
B-50-12.9-MTO-100	15, 16, 17, 18	60.6	5.2	-36.2	-30.6	-20.9	1.91	6.5
B-50-12.9-MTO-150	26, 27, 28, 29	56.7	3.5	-31.8	-25.7	-15.4	1.93	11.5
B-50-12.9-C(T)O-50	8, 9, 10	19.6	11.1	97.4	114.9	144.8	0.19	8.2
B-50-12.9-C(T)O-100	19, 20, 21, 22	61.1	3.8	-36.6	-31.0	-21.4	1.66	17.9
B-50-12.9-CO-150	30, 31, 32	59.6	4.7	-35.0	-29.3	-19.5	2.21	8.7
B-50-S355-CO-50	33, 34, 35	21.6	5.8	79.4	95.2	122.4	0.25	18.1
B-50-S355-CO-100	36, 37, 38, 39	57.5	9.8	-32.7	-26.7	-16.5	1.74	18.8
B-50-S355-CO-150	40, 41, 42	59.2	11.6	-34.6	-28.8	-18.9	2.19	47.2

[a] Mean value and CoV of δ_{peak} not significant for excess of scatter;

[b] $Diff_1 = 100 \times \left(F_{Rk} - \overline{F}_{peak}\right) / \overline{F}_{peak}$, with F_{Rk} computed for ρ_k = 680 kg/m^3;

[c] $Diff_2 = 100 \times \left(F_{Rm} - \overline{F}_{peak}\right) / \overline{F}_{peak}$, with F_{Rm} computed for ρ_m = 740 kg/m^3;

[d] $Diff_3 = 100 \times \left(F_{Rm,meas} - \overline{F}_{peak}\right) / \overline{F}_{peak}$, with $F_{Rm,meas}$ computed for $\rho_{m,meas}$ = 843 kg/m^3.